MOLECULAR AND CELLULAR BIOLOGY, Feb. 2008, p. 1068–1080 Vol. 28, No. 3
0270-7306/08/$08.00+0 doi:10.1128/MCB.00484-07

A Non-Tumor Suppressor Role for Basal p19^{ARF} in Maintaining Nucleolar Structure and Function▽

Anthony J. Apicelli,[1,2] Leonard B. Maggi, Jr.,[1,2] Angela C. Hirbe,[1] Alexander P. Miceli,[1,2] Mary E. Olanich,[1,2] Crystal L. Schulte-Winkeler,[1,2] Anthony J. Saporita,[1,2,3] Michael Kuchenreuther,[1,2,3] José Sanchez,[1,2] Katherine Weilbaecher,[1,3] and Jason D. Weber[1,2,3]*

Departments of Internal Medicine,[1] Division of Molecular Oncology, and Cell Biology and Physiology,[2] and Cancer Biology Pathway,[3] Siteman Cancer Center, Washington University School of Medicine, St. Louis, Missouri 63110

Received 20 March 2007/Returned for modification 11 May 2007/Accepted 14 November 2007

The nucleolus is the center of ribosome synthesis, with the nucleophosmin (NPM) and p19^{ARF} proteins antagonizing one another to either promote or inhibit growth. However, basal NPM and ARF proteins form nucleolar complexes whose functions remain unknown. Nucleoli from *Arf*$^{-/-}$ cells displayed increased nucleolar area, suggesting that basal ARF might regulate key nucleolar functions. Concordantly, ribosome biogenesis and protein synthesis were dramatically elevated in the absence of *Arf*, causing these cells to exhibit tremendous gains in protein amounts and increases in cell volume. The transcription of ribosomal DNA (rDNA), the processing of nascent rRNA molecules, and the nuclear export of ribosomes were all increased in the absence of ARF. Similar results were obtained using targeted lentiviral RNA interference of ARF in wild-type MEFs. Postmitotic osteoclasts from *Arf*-null mice exhibited hyperactivity in vitro and in vivo, demonstrating a physiological function for basal ARF. Moreover, the knockdown of NPM blocked the increases in *Arf*$^{-/-}$ ribosome output and osteoclast activity, demonstrating that these gains require NPM. Thus, basal ARF proteins act as a monitor of steady-state ribosome biogenesis and growth independent of their ability to prevent unwarranted hyperproliferation.

Cellular growth (i.e., macromolecular synthesis) is an essential function during the early parts of the cell cycle. For cells to transit the G_1 restriction point, they must duplicate nearly their entire protein content; failure to do so would result in smaller daughter cells (12). Only recently has an emphasis been placed on the fundamental control of cell growth and its link to the cell cycle. Developments in the understanding of how the cell senses environmental nutritional cues has led to a flurry of research on understanding the mechanisms underlying growth control (40). Not surprisingly, several of these pathways converge on the synthesis of new ribosomes in the cell nucleolus and the regulation of translation.

Approximately half of the cell's energy expenditure is directed toward ribosome biogenesis (26). The nucleolus, long recognized as a marker for active cellular growth, was first described in the early 1960s as the center of ribosomal DNA (rDNA) transcription and ribosome biogenesis (6, 32). This organelle is composed of three regions, on the basis of morphology at the ultrastructural level: the fibrillar centers, the dense fibrillar compartment, and the granular zone. rDNA transcription occurs in the junction region between the fibrillar centers and the surrounding dense fibrillar component, and the resulting rRNA is further processed in the periphery of the dense fibrillar component. Further posttranscriptional modifications and assembly into subunits occur in the surrounding granular region (18).

While the primary mechanisms regulating these processes have been well studied in *Saccharomyces cerevisiae* (13), multicellular organisms demand more complex regulatory mechanisms, in that proliferative capacity is determined not only by the relative abundance of nutrients but also by complicated extracellular signals and growth factors. Indeed, previous studies have demonstrated convergence between the growth and the proliferation pathways via regulation of the tumor suppressor gene products Rb and p53 (9, 17, 43, 48). Both products are known to negatively regulate the activity of polymerase I in rDNA transcription. Oncogenes such as c-Myc also regulate the transcription of rDNA and the genes that encode ribosomal proteins, implying that an intricate network exists within the nucleolus to ensure the proper synthesis of ribosomes (7, 15, 16).

The tumor suppressor p19^{ARF} represents an attractive candidate for coupling proliferation to growth. Given its nucleolar localization (39, 44, 45) and potent induction by hyperproliferative signals (19, 20, 31, 50), ARF represents a potential nucleolar integrator of growth signals coming into the cell. It has been regarded classically as an activator of p53 through its ability to sequester Mdm2, the E3 ubiquitin ligase for p53, in the nucleolus (39, 44, 45). However, recent data have demonstrated a role for ARF in binding to and affecting the function of the ribosomal chaperone nucleophosmin (NPM), independent of its ability to regulate p53 (4, 8, 21). Furthermore, these data are consistent with those from a growing number of studies with mice and humans that describe p53-independent functions for ARF tumor suppression (35).

* Corresponding author. Mailing address: Department of Internal Medicine, Division of Molecular Oncology, Washington University School of Medicine, Campus Box 8069, 660 S. Euclid Avenue, St. Louis, MO 63110. Phone: (314) 747-3896. Fax: (314) 747-2797. E-mail: jweber@im.wustl.edu.

▽ Published ahead of print on 10 December 2007.

Given ARF's nucleolar localization, its role in suppressing cellular growth and proliferation, and its ability to bind to a protein involved in ribosome biogenesis, we were inclined to explore the functional and physiological consequences of ARF disruption of growth and ribosome biogenesis. Through in vitro and in vivo assays, we utilized targeted *Arf* knockout mice and selective ARF knockdown via lentiviral RNA interference. Cells derived from *Arf*-null mice displayed significant alterations in gross nucleolar morphology and abundance and had a marked increase in basal protein synthesis levels compared to that in wild-type cells. Furthermore, this increase in protein synthesis was correlated to increased ribosome biogenesis and cytoplasmic ribosome content, implying a regulatory role for ARF in these processes. Importantly, though ARF levels are nearly undetectable in low-passage mouse embryonic fibroblasts (19), the knockdown of endogenous ARF via short hairpin RNA (shRNA) constructs mimicked the *Arf*-null nucleolar and ribosomal phenotype, implying an important ribosome homeostatic role for basal ARF proteins in wild-type cells. The progrowth phenotype of the *Arf* loss was not limited to proliferating cells, as fully differentiated osteoclasts from *Arf*-null mice exhibited tremendous gains in protein synthesis and overall activity in vivo. Mechanistically, all of the ribosome gains exhibited by the loss of *Arf* were reversed by the removal of the nucleolar NPM proto-oncogene, indicating that NPM, when untethered from ARF, promotes unrestrained ribosome biogenesis. Taken together, these data strongly argue for a moment-to-moment "thermostat"-like role for basal ARF molecules in controlling NPM-directed ribosome biogenesis and protein synthetic rates.

MATERIALS AND METHODS

Mice. $Arf^{-/-}$ mice were rederived from triple-knockout heterozygous mice ($Arf^{+/-}$ $Mdm2^{+/-}$ $p53^{+/-}$; a generous gift from G. Zambetti, St. Jude, Memphis, TN) to a pure C57BL/6 background by several generations of backcrosses to wild-type C57BL/6 mice, followed by breeding to homozygosity. Age-matched wild-type C57BL/6 littermates were used as controls where indicated. Organs were harvested from mice 4 days postnatally.

Cell culture, reagents, and antibodies. Low-passage (2–5) MEFs were isolated and maintained in Dulbecco's modified Eagle's medium supplemented with 10% fetal bovine serum, 10 μg/ml gentamicin, 1× nonessential amino acids, 1 mM sodium pyruvate, and 2 mM glutamine. Rabbit anti-p16INK4A (sc-1207), goat anti-γ-tubulin (catalog no. sc-7396), and rabbit anti-Myc (catalog no. sc-764) were purchased from Santa Cruz Biotechnology. Rat anti-$p19^{ARF}$ (catalog no. NB 200-169A) was purchased from Novus Biologicals. Mouse anti-NPM (catalog no. 32-5200) was purchased from Zymed.

Plasmid constructs. pLKO-GFP, a lentiviral shRNA expression vector was a generous gift from Sheila Stewart (Washington University). To construct the ARF shRNA vector, pLKO-GFP was digested with AgeI/MluI, and annealed oligonucleotides containing the shRNA target (nucleotides 157 to 177 of exon 1β of $p19^{ARF}$) or a scrambled control were cloned into these sites. The resultant clones were verified by sequencing. The oligonucleotides used were small interfering ARF (siARF) sense (5′-CCGGGCTCTGGCTTTCGTGAACATGCTCGAGCATGTTCACGAAAGCCAGAGCTTTTTA-3′), siARF antisense (5′-CGCGTAAAAAGCTCTGGCTTTCGTGAACATGCTCGAG CATGTTCACGAAAGCCAGAGC-3′), siScrambled sense (5′-CCGGTACG ACCTGAACTGCTTAGGACTCGAGTCCTAAGCAGTTCAGGTCGTATTTTTA-3′), and siScrambled antisense (5′-CGCGTAAAAATACGACCTGAACTGCTTAGGACTCGAGTCCTAAGCAGTTCAGGTCGTA-3′). The underlined portions represent the 21 nucleotide hairpin sense and antisense strands. For NPM knockdown, annealed oligonucleotides were cloned as described above into pLKO-GFP, the sequences of which were previously reported (27). RNA interference for endogenous c-Myc was performed with siRNAs recognizing the 3′ untranslated region (UTR) of c-Myc (5′-AACGTTTATAACAGTTACAAA-3′ [Qiagen]). Myc-ER retrovirus was generated and used to infect wild-type and *Arf*-null MEFs as previously described (50).

AgNOR staining. MEFs were seeded onto glass coverslips overnight and were fixed and stained the following day. A silver nucleolar organizing region (AgNOR) staining method was modified from the protocol presented by Aubele et al. (1). Briefly, cells were fixed in 2% glutaraldehyde, followed by a postfixation in a 3:1 ethanol-acetic acid solution. Cells were stained with a 0.33% formic acid-33.3% silver nitrate solution in 0.66% gelatin and mounted on slides with Vectashield (Vector Labs).

Histomorphometry. Histomorphometric analysis was performed with OsteoQuant Nova Prime software (Bioquant Image Analysis Corp.) on images captured at ×200 magnification by an Optitronics Magnifire camera on a Nikon TE300 microscope. Total numbers and total areas (μm^2) of AgNOR regions per nucleus from 100 nuclei were assessed, and statistical significance was determined using Student's *t* test.

Electron microscopy. Asynchronously growing wild-type and $Arf^{-/-}$ MEFs were trypsinized and fixed with 2% glutaraldehyde in phosphate-buffered saline for 10 min. Samples were further processed by the Washington University Department of Cell Biology's Electron Microscopy Core. Pictures of nuclei and nucleoli were taken at magnifications of ×3,000 and ×7,000, respectively.

[^{35}S]methionine incorporation assay. Cells (1×10^5) were seeded in triplicate and then starved of methionine and cysteine. Cells were pulsed with 14.3 μCi of [^{35}S]methionine (Amersham) and then immediately washed twice with cold phosphate-buffered saline and lysed with 1% Triton X-100 buffer. Total protein was precipitated from lysates with 10% trichloroacetic acid. Pellets were subjected to liquid scintillation counting to measure the incorporated counts per minute.

Ribosome fractionation. Cells (2×10^6) were treated with 50 μg/ml cycloheximide prior to trypsinization and lysis, and fractionation was carried out over a 10 to 45% sucrose gradient (46). Gradients were fractionated, and RNA absorbance at 254 nm was monitored continuously to detect ribosomal subunits.

Lentiviral production and infection. 293T cells (5×10^5) were transfected with 1 μg of pLKO-GFP containing either scrambled or ARF shRNA cassettes along with the pHR8.2ΔR packaging vector and the pCMV-VSV-G envelope vector. Viral supernatants were collected and pooled. Wild-type MEFs (8×10^5) were plated and infected with viral supernatant containing 10 μg/ml protamine sulfate. Cells were infected again on the following day, checked for green fluorescent protein expression, and allowed to express the shRNA construct for 48 h.

Serum assays. Levels of tartrate-resistant acid phosphatase (TRAP) 5b were measured in serum collected from wild-type or $Arf^{-/-}$ mice, using a TRAP 5b enzyme-linked immunosorbent assay (ELISA) system (IDS, Fountain Hills, AZ).

Osteoclast formation assays. Whole bone marrow was extracted from femurs and tibias of wild-type or $Arf^{-/-}$ mice and plated in CMG-14-12 culture supernatant (1/10 vol) in α-minimal essential medium (α-MEM) containing 10% fetal calf serum (FCS) to generate primary bone marrow macrophages (BMM), as described previously (49). Cells were fed every day with α-MEM containing 10% FCS, CMG-14-12 supernatant (1/20 vol), and glutathione *S*-transferase-RANK ligand (GST-RANKL) (100 ng/ml) and incubated for 5 days to generate osteoclasts (49). TRAP staining was performed according to the manufacturer's instructions (Sigma-Aldrich, St. Louis, MO). Five fields at a magnification of ×4 were captured with the Magnafire system, and the TRAP-positive cells with three or more nuclei were counted by one blinded to the genotype. A quantitative TRAP solution assay was performed by adding a colorimetric substrate, 5.5 mM *p*-nitrophenyl phosphate, in the presence of 10 mM sodium tartrate at pH 4.5.

Macrophage proliferation assays. BMMs (1×10^4) were plated in α-MEM containing 10% FCS and CMG-14-12 supernatant (1/10 vol). Cells were starved in α-MEM containing 0.1% FCS for 12 h. At this time, α-MEM containing 10% FCS and CMG-14-12 supernatant (1/10 vol) was added back to the cells. Cells were labeled with bromodeoxyuridine (BrdU) for 24 h, and proliferation was measured using the chemiluminescent cell proliferation ELISA (Roche Diagnostics, Mannheim, Germany).

Western blotting and serial immunoprecipitation. MEF cell extracts (30 μg) were loaded onto 4 to 20% sodium dodecyl sulfate (SDS)-polyacrylamide gels (ISC Biosciences), transferred to polyvinylidene difluoride membrane (Millipore), and probed with antibody to rat anti-$p19^{ARF}$ (Novus Biologicals), goat anti-γ-tubulin (Santa Cruz Biotechnology), rabbit anti-Myc (Santa Cruz Biotechnology), rabbit anti-p16INK4A (Santa Cruz Biotechnology), and rabbit anti-L5 (ILAMM). Secondary horseradish peroxidase-conjugated anti-rabbit, anti-goat, or anti-rat antibodies (Jackson ImmunoResearch) and ECL+ (Amersham) were used to visualize the bands. For serial immunoprecipitation, 200 μg of wild-type MEF lysate was immunoprecipitated with GammaBind (Amersham) by a custom-made rabbit NPM polyclonal antibody (Sigma Genosys) (46). The final supernatant was concentrated with a Vivaspin column (Vivascience), and all

samples were loaded onto 10% SDS-polyacrylamide gels for immunoblotting analysis.

47S rRNA real-time reverse transcription-PCR. Levels of 47S rRNA transcripts were determined as described previously by Cui and Tseng (10). Briefly, total RNA was reverse transcribed with a mouse rRNA-specific primer (5′-CG TGGCATGAACACTTGG-3′). Real-time PCR was performed with iQ SYBR Green Supermix (Bio-Rad) according to the manufacturer's protocol, with the forward primer 5′-CTGACACGCTGTCCTTTCCC-3′ and the reverse primer 5′-GTGAGCCGAAATAAGGTGGC-3′ on an iCycler thermal cycler (Bio-Rad). The absolute copy number was obtained by comparison to serial dilutions of a known amount of plasmid containing the mouse rDNA repeat.

rRNA labeling experiments. Equal numbers of wild-type and $Arf^{-/-}$ MEFs were starved in methionine-free media containing 10% dialyzed fetal bovine serum. For uridine labeling, cells were labeled in medium containing 2.5 μCi/ml [^{3}H]uridine (Amersham) and then chased in label-free medium. Where noted, cells were treated with 50 μCi/ml [*methyl*-^{3}H]methionine (Amersham) for 30 min and chased in unlabeled methionine-containing (10 μM) media in the nuclear/cytoplasmic fractionation experiments. Total RNA was isolated using Trizol reagent (Invitrogen) and loaded onto 1% agarose-formaldehyde gels for the uridine experiments. Cellular fractionation was carried out using a nuclear extraction kit according to the manufacturer's protocol (Active Motif). Total RNA was isolated from the nuclear and cytoplasmic fractions using Trizol and loaded onto 1% agarose-formaldehyde gels. RNA was transferred to Hybond N+ membranes (Amersham), cross-linked, sprayed with En^{3}Hance (Perkin-Elmer), and subjected to autoradiography.

RESULTS

p19^{ARF} is required for proper nucleolar morphology. A common theme in ARF biology is its intrinsic localization within the nucleolus, under both basal and oncogene-induced settings (31, 39, 44, 45). Many of ARF's binding partners either reside in the nucleolus or are relocalized there by ARF itself (25, 35). Of the resident nucleolar ARF binding proteins, nearly all are involved in some facet of ribosome biogenesis (e.g., transcription, processing, or export) (34, 35). We hypothesized that basal nucleolar ARF proteins, even at low levels, might exert a subtle activity on these nucleolar proteins to continuously monitor their function. To this end, we adapted an AgNOR staining protocol (1) for use with MEFs derived from wild-type and from $Arf^{-/-}$ mice. Staining methods utilizing the reduction of silver on argyrophilic proteins surrounding the nucleolar organizing region have been used for decades as a prognostic factor with certain carcinomas, wherein increases of the AgNOR index tend to correlate with poor prognoses (28). AgNOR staining of $Arf^{-/-}$ MEFs demonstrated markedly higher numbers of AgNORs per nucleus and a distinctly irregular shape than the numbers and the more rounded, symmetrical shape of the wild-type AgNOR counterparts (Fig. 1A). At the ultrastructural level, we also observed multiple, elongated, irregular nucleoli in $Arf^{-/-}$ cells compared to the round nucleoli of the wild-type cells (Fig. 1B, top panels). These irregularities in *Arf*-null cells were also associated with larger fibrillar centers, the sites of rDNA transcription (Fig. 1B, bottom panel, arrows). We quantitated the total nucleolar area per nucleus (a common pathological definition of the AgNOR index) (42) and observed a 20% increase in $Arf^{-/-}$ cells (31.6 μm^2 versus 26.4 μm^2; $n = 100$; $P < 0.001$) (Fig. 1C). A significant increase in the AgNOR number per nucleus was also observed (5.78 versus 3.49; $n = 100$; $P < 0.001$). Additionally, nucleolar morphology changes were observed in vivo. Intestine and liver tissues harvested from newborn wild-type and *Arf*-null mice and stained for AgNORs recapitulated our earlier in vitro findings in that the loss of *Arf* resulted in dramatic gains in both AgNOR numbers and overall area (Fig. 2A and B). Moreover, we also observed a moderate increase in the number of larger multinucleolar cells in the livers of *Arf*-deficient mice (Fig. 2A, right panels). Taken together, these data suggest a role for p19^{ARF} in maintaining a proper nucleolar structure in vitro and in vivo.

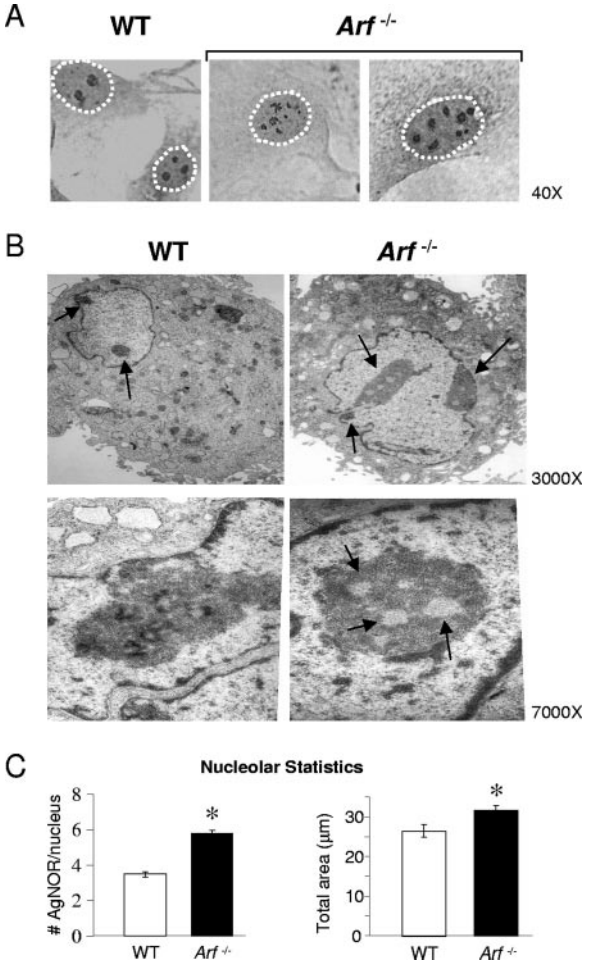

FIG. 1. Loss of ARF results in nucleolar morphological changes. (A) AgNOR staining of representative wild-type (WT) and $Arf^{-/-}$ MEFs. Increases in the number and irregularity of the AgNOR indices in the $Arf^{-/-}$ cells are shown. (B) Ultrastructural features of nuclei from the wild-type and $Arf^{-/-}$ MEFs. Arrows indicate nucleoli (×3,000) and fibrillar centers (×7,000). (C) Quantification of AgNOR indices from panel A. The left panel shows the number of AgNORs per nucleus ($n = 100$). The right panel shows the total nucleolar area (in μm^2) per nucleus as determined by histomorphometric analysis ($n = 100$). *, $P < 0.01$.

Loss of *Arf* enhances protein synthesis and ribosome biogenesis independent of proliferation. The loss of *Arf* resulted in dramatic alterations in nucleolar structure (Fig. 1 and 2), suggesting that basal ARF may function in the maintenance of this organelle. To determine whether changes in nucleolar structure result in altered nucleolar function, we assessed ribosome output from the nucleolus. First, we performed [^{35}S]methionine pulse-labeling experiments, measuring the amount of radioactivity incorporated into newly translated proteins over time. As shown, $Arf^{-/-}$ MEFs had an approxi-

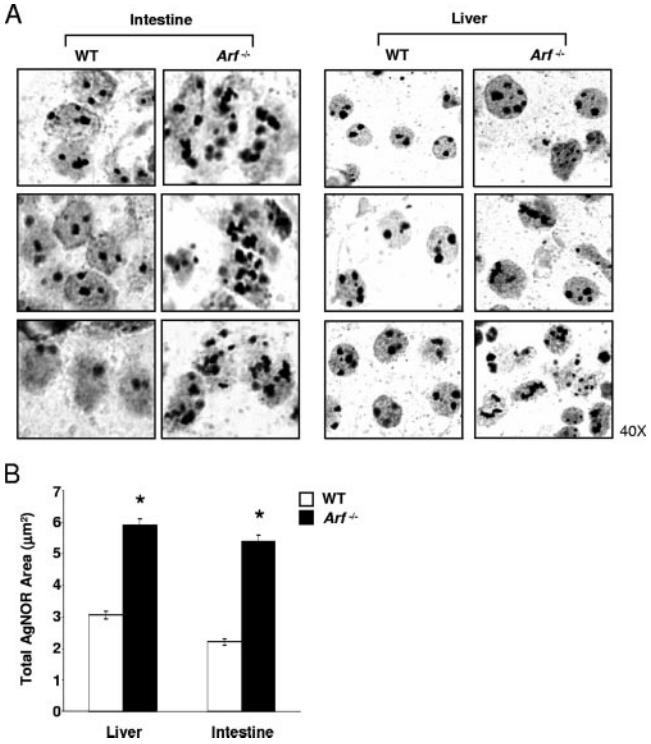

FIG. 2. Tissues from newborn $Arf^{-/-}$ mice display altered nucleolar morphology reminiscent of the in vitro findings. (A) AgNOR staining of representative sections from the intestine and liver. (B) Quantification of total AgNOR area per nucleus ($n = 100$). *, $P < 0.01$. WT, wild type.

mately fourfold increase in incorporated [^{35}S]methionine compared to that of wild-type cells after 24 h (Fig. 3A). Furthermore, this increased protein synthesis was not related to any increase in proliferation rates, as the proliferation of the low-passage wild-type and the $Arf^{-/-}$ MEFs was virtually identical (Fig. 3B). To determine if the protein synthesis differences were due to increased ribosomal output, we performed sucrose density gradient rate-zonal ultracentrifugation of cytoplasmic lysates from wild-type and *Arf*-null cells to separate ribosomes. Ribosome subunits and actively translating polysomes were identified by real-time monitoring of absorbance at 254 nm to detect the relative amounts of ribosomal RNAs present in each of the subunit fractions. Compared to the wild-type lysates, lysates of the $Arf^{-/-}$ cells had significantly more (nearly 40%) cumulative absorbance in the actively translating polysome fraction, indicating a relative abundance of these ribosomal components (Fig. 3C). Consistent with gains in ribosome production and protein synthesis, we observed a significant increase in the overall volume of low-passage *Arf*-deficient MEFs as well as a robust increase in protein content per cell (Fig. 3D and E). Moreover, gains in ribosome biogenesis were also seen in vivo. Livers were isolated from newborn wild-type and *Arf*-null mice, minced, and immediately placed in [^{35}S]methionine-containing medium to measure protein synthesis rates. Cells isolated from *Arf*-null livers exhibited a nearly 15-fold increase in protein synthesis compared to that of the wild-type littermates (Fig. 4A). Additionally, cells freshly isolated from $Arf^{-/-}$ mouse spleens also showed dramatic increases in 40S, 60S, and 80S and polysome content (Fig. 4B), demonstrating elevated ribosome output in these tissues. We therefore postulated that basal ARF proteins might act as negative regulators at a certain step(s) in nucleolar ribosome biogenesis.

The acute knockdown of ARF mimics the phenotype of $Arf^{-/-}$ cells. Since ARF's role in sensing hyperproliferative signals and concomitantly inducing p53-dependent cell cycle arrest have been well established (19, 20, 31, 50), it has been assumed that basal ARF has little, if any, function in the normal day-to-day regulation of cellular homeostasis. However, ARF levels in asynchronously growing wild-type cells are detectable by Western blotting analysis and immunohistochemistry (5). Given our finding that $Arf^{-/-}$ cells exhibit chronic nucleolar morphology changes and increased ribosome output (Fig. 1 to 4), we were poised to reexamine this question in an acute setting by knocking down basal ARF in wild-type cells. This was accomplished by using lentiviral constructs containing a shRNA duplex that recognized bases 157 through 177 in the ARF-specific exon 1β of the *Ink4a/Arf* locus. To verify the specificity of this construct, we infected wild-type MEFs with lentivirus containing either shRNA specific to ARF or a scrambled control sequence. As shown by Western blotting analysis, infection with viruses containing the ARF shRNA sequence produced a robust knockdown of the level of ARF (96%) without decreasing levels of p16INK4A (Fig. 5A). Moreover, expression of other nucleolar proteins, such as NPM and ribosomal protein L5, also remained unchanged following the ARF knockdown (Fig. 5A). As observed first with the $Arf^{-/-}$ MEFs, the ARF knockdown MEFs also exhibited dramatic nucleolar morphology alterations as depicted by AgNOR staining (Fig. 5B). These acute changes were of greater statistical difference than those originally observed with *Arf*-null cells, with a significant increase in both the number of AgNORs per nucleus (6.6 versus 3.3; $n = 100$; $P < 0.001$) and the total AgNOR-stained area per nucleus (49.8 μm^2 versus 36.8 μm^2; $n = 100$; $P < 0.001$) (Fig. 5C). Similarly, the ARF knockdown MEFs displayed tremendous gains in protein synthesis rates as determined by [^{35}S]methionine incorporation, nearly 10-fold higher than that of scrambled control MEFs (Fig. 5D) and almost twice as high as that of *Arf*-null MEFs (compared to Fig. 3A). The ARF knockdown MEFS also produced significantly more actively translating polysomes (55% more) as determined by UV monitoring of cytosolic rRNAs (Fig. 5E), suggesting that the acute loss of ARF has a greater impact on nucleolar functions.

Genetic disruption of *Arf* results in increased osteoclast numbers in vitro and elevated levels of TRAP protein in vitro and in vivo. To demonstrate a physiological function for ARF's baseline regulation of ribosome biogenesis and protein synthesis, we focused on bone-resorbing osteoclasts as a model of a differentiated cell with high protein synthesis demands. Osteoclasts are formed by the fusion of hematopoietically derived macrophages into multinucleated giant cells with a specialized ruffled border containing thousands of vacuolar H^+-ATPases. The osteoclast forms a sealing zone against the area of bone resorption and, in doing so, allows the specialized ruffled membrane to secrete collagenase and dramatically lower the pH through the activity of the proton pumps. As a result, the osteoclast has a high demand for protein synthesis, since the H^+-ATPases are specific to the mature osteoclast and are not

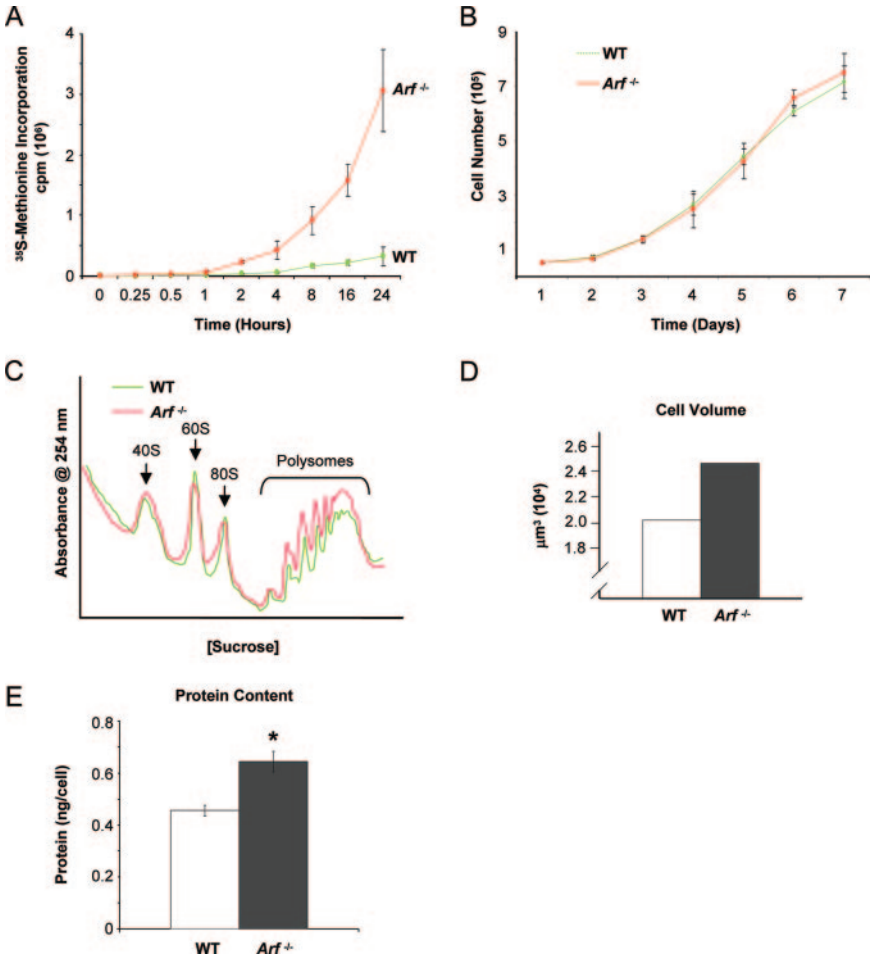

FIG. 3. Disruption of ARF enhances protein synthesis independent of cellular proliferation. (A) Cells were starved of methionine and cysteine for 30 min prior to the addition of a [^{35}S]methionine label for the indicated times, followed by lysis, trichloroacetic acid precipitation of proteins, and liquid scintillation counting. (B) Equal numbers of cells (1×10^5) were plated in triplicate at day 0 and then were trypsinized and counted via a hemocytometer at various time points. (C) Cycloheximide (50 μg/ml) was added for 10 min prior to lysis and ultracentrifugation of cleared lysate on 10 to 40% sucrose gradients. The graph shows an A_{254} of ribosome subunits over increasing sucrose density. (D) Equal-passage MEFs (1×10^5) were trypsinized and analyzed by a Coulter Vi-Cell counter for cell volume. (E) Equal-passage MEFs (1×10^6) were harvested and analyzed for protein content by a standard colorimetric DC assay. WT, wild type.

found in macrophage precursors (41). Furthermore, since the mature osteoclast is a postmitotic cell, it affords an excellent opportunity to examine ARF's effects on protein and ribosome metabolism independent of proliferation.

We first determined whether the proliferation rates varied between wild-type and $Arf^{-/-}$ BMM, osteoclast precursors. BrdU labeling of BMMs demonstrated no significant differences in the proliferation rates between wild-type and $Arf^{-/-}$ osteoclast precursors (Fig. 6A), similar to the equal proliferation rates of early passage MEFs (Fig. 3B). Next, BMMs from $Arf^{-/-}$ and wild-type mice were induced to produce mature osteoclasts by the addition of macrophage colony-stimulating factor (M-CSF) and RANKL. After 3 days of stimulation with RANKL, cells were fixed and stained with a TRAP substrate, an osteoclast-specific stain that relies on the abundance of TRAP protein produced by the osteoclast. An increased number of mature osteoclasts derived from the $Arf^{-/-}$ precursors was observed compared to that of the wild-type controls (Fig. 6B). TRAP-positive cells with greater than five nuclei were counted as a way to differentiate maturing osteoclasts from immature precursors and resulted in a significant increase in the $Arf^{-/-}$ genotype (149 versus 91 per well; $n = 5$; $P = 0.01$) (Fig. 6C).

To determine if the differences seen with osteoclastogenesis were functionally relevant, we compared the TRAP activities (a marker of osteoclast function) of equal numbers of TRAP-positive cells, as determined above. Cell lysates were incubated from day 4 post-RANKL addition (for wild-type cells) and day 3 post-RANKL addition (for $Arf^{-/-}$ cells), where approximately equal numbers of multinucleated TRAP-positive cells were observed, with *p*-nitrophenyl phosphate, a colorimetric substrate for TRAP. A twofold increase in TRAP activity was seen with *Arf*-null cells compared to that with wild-type cells ($P < 0.01$) (Fig. 6D), indicating that the $Arf^{-/-}$ osteoclasts are far more active than their wild-type counterparts on a per cell basis. In vivo analysis of osteoclast function of *Arf*-null mice mimicked our in vitro findings of osteoclast hyperactivity, as there was an 18% increase in the level of

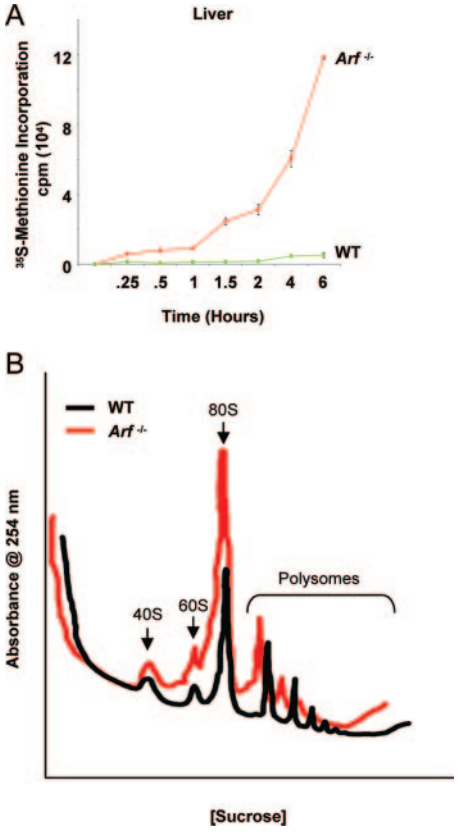

FIG. 4. ARF regulates protein synthesis and ribosome biogenesis in vivo. (A) Livers were isolated from three wild-type (WT) and *Arf*-null littermates and briefly trypsinized. Cells (5×10^6) were immediately cultured in methionine-free medium for 15 min and then incubated with [^{35}S]methionine for the indicated times. Proteins were trichloroacetic acid precipitated, and labeled proteins were quantified by liquid scintillation counting. (B) Spleens were isolated from three wild-type and *Arf*-null littermates. Cells (1×10^7) were immediately harvested, and cytosolic fractions were loaded onto 7 to 47% sucrose gradients for ultracentrifugation separation. Graph B shows an A_{254} of ribosome subunits over increasing sucrose density.

serum TRAP activity over that of the wild type controls (Fig. 6E).

Loss of *Arf* increases rRNA transcription, rRNA processing, and ribosome nuclear export. Previous reports have demonstrated a role for ARF in rRNA processing (37). Furthermore, our laboratory has previously demonstrated ARF's inhibitory activity on the shuttling of NPM (8) and NPM's nucleolar cargo, rpL5 and 5S rRNA (46). Additional reports have demonstrated a role for nucleolar ARF in preventing rDNA transcription through both Myc-dependent and -independent mechanisms (2, 3, 30). Taken together, nucleolar ARF could prevent all three steps in ribosome biogenesis: transcription, processing, and export. The loss of *Arf* had no impact on the levels of either NPM or rpL5, suggesting that ARF's effect on this pathway was not due to altered synthesis and/or destruction of these proteins (Fig. 7A). Moreover, serial immunodepletion of NPM revealed two distinct pools of ARF: one that is effectively associated with NPM (Fig. 7B, lane 1) and a second pool that is free from NPM (Fig. 7B, lane 6). This implies that ARF's effects on ribosome biogenesis may not be relegated to only NPM-dependent processes and is consistent with the idea that ARF antagonizes rDNA transcription through other unique, physically interacting proteins. Accordingly, the loss of *Arf* resulted in a fourfold increase in 47S rRNA transcription (Fig. 7C), a process thought to be independent of direct NPM regulation (as NPM does not localize to the fibrillar compartment of the nucleolus).

Newly transcribed 47S rRNAs are further processed in the nucleolus into their mature 28S, 18S, and 5.8S rRNAs (34). These processes are known to be readily antagonized by overexpressed ARF (37). To determine the effect of the *Arf* loss on these events, newly synthesized 47S rRNAs were followed through nucleolar processing. rRNA processing was greatly accentuated in the $Arf^{-/-}$ MEFs over a 2-h period (Fig. 7D). While the wild-type and the *Arf*-null cells clearly start with different amounts of 47S rRNA (Fig. 7C), the *Arf*-null cells are capable of churning out more processed rRNAs (15-fold more than the wild type), which is nearly a threefold amplification over the starting amount of 47S transcripts. This suggests that while levels of 47S rRNA are certainly permissive for greater processing of rRNAs, they cannot entirely account for the sheer magnitude of increases in processed rRNAs observed in the $Arf^{-/-}$ cells.

To determine the precise step at which ARF might influence rRNA processing, we labeled cells with [*methyl*-^{3}H]methionine, which labels rRNA, and loaded equal amounts of the radioactive label to examine processing intermediates after short time periods of chase with label-free media. We observed only a modest increase of the 32S rRNA precursors in cells lacking *Arf* at early time periods, indicating that ARF may interfere with the processing steps between the 47S transcript and the 32S intermediate (Fig. 7E). However, after 2 h of chase, we saw no differences in the relative amounts of radioactivity in the final 18S and the 28S products, indicating that the loss of *Arf* had no impact on these downstream processing steps. These results exactly mirror what Sugimoto and colleagues observed when they overexpressed ARF, namely, an accumulation of improperly processed rRNA intermediates between the 47S and 32S stages (37), albeit to a far lesser extent in our experiments.

As a final step in ribosome biogenesis, mature ribosome subunits are exported to the cytosol in a process that we have previously attributed to NPM-directed nuclear export (27, 46). The *Arf*-null MEFs exhibited a more robust (~25-fold) nuclear export of newly processed rRNAs than the wild-type cells did (Fig. 8A). Again, this extreme difference between the wild-type and the *Arf*-null cells was far greater than any previous step in ribosome biogenesis (e.g., transcription or processing), implying that each step represents an amplification of the previous step. This was most evident when the real-time nuclear export of rRNAs, as monitored by scintillation counting of newly exported ^{3}H-labeled rRNA, revealed that the absolute rates of rRNA export were threefold increased in cells lacking *Arf* (Fig. 8B). Taking these data together, we believe this reflects the ability of ARF to regulate moment-to-moment steps in ribosome biogenesis, such that alterations in ARF levels may produce robust and rapid responses that effect cytoplasmic ribosomal content.

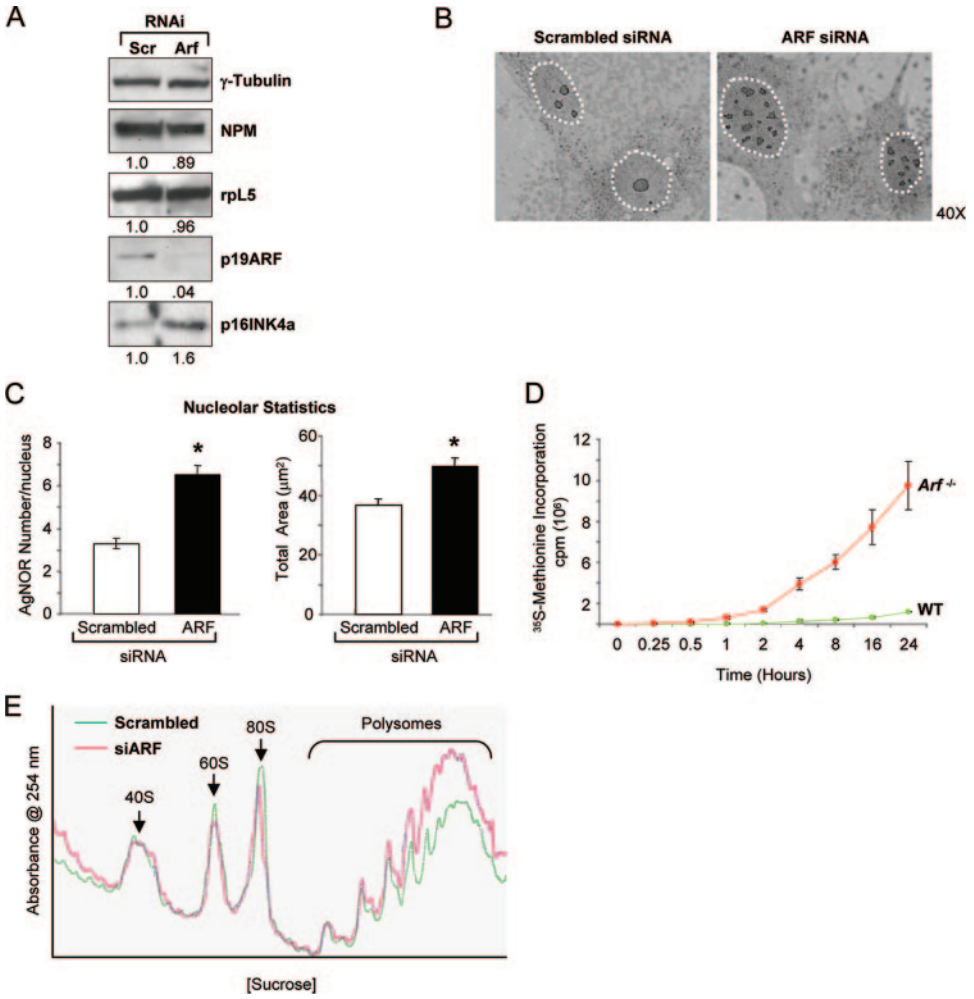

FIG. 5. Acute depletion of $p19^{ARF}$ results in nucleolar, morphological, and functional changes reminiscent of the $Arf^{-/-}$ cells. (A) Western blotting confirmation of the $p19^{ARF}$ knockdown in wild-type (WT) MEFs 96 h postinfection with lentiviral shRNA constructs using antibodies recognizing γ-tubulin, NPM, rpL5, $p19^{ARF}$, and p16INK4a. Expression change (*n*-fold) is marked under each panel. (B) AgNOR staining of representative MEFs infected with control (scrambled) or $p19^{ARF}$-specific shRNA virus. (C) Quantification of AgNOR indices. Left panel shows the number of AgNORs per nucleus ($n = 100$). Right panel shows the total nucleolar area (in μm^2) per nucleus as determined by histomorphometric analysis ($n = 100$). *, $P < 0.01$ (D) Total radioactivity incorporated after [^{35}S]methionine pulse. Cells were starved of methionine and cysteine for 30 min prior to the addition of label for the indicated times, followed by lysis, trichloroacetic acid precipitation of proteins, and liquid scintillation counting. (E) Cycloheximide (50 μg/ml) was added for 10 min prior to lysis and ultracentrifugation of cleared lysate on 10 to 40% sucrose gradients. The graph shows an A_{254} of ribosome subunits over increasing sucrose density.

Myc is not responsible for the rDNA transcription increases in the $Arf^{-/-}$ cells. Previous reports have shown that the c-Myc transcription factor, in part, localizes to the nucleolus to positively regulate the transcription of rDNA (15, 16). Moreover, ARF has been shown to antagonize Myc functions through direct interactions (30). Thus, we sought to determine whether basal ARF proteins might be regulating nucleolar Myc to prevent the aberrant transcription of the rDNA loci. We utilized siRNAs targeting the 3′ UTR of c-Myc to successfully knock down endogenous Myc nearly 20-fold (Fig. 9A). While lower Myc protein levels greatly reduced 47S rRNA transcripts in wild-type MEFs, it had little impact on 47S copies in the $Arf^{-/-}$ MEFs (Fig. 9B). While the former result is consistent with previous studies showing a role for Myc in rDNA transcription (15, 16), the latter result suggests that Myc is not absolutely required for rDNA transcription in cells lacking *Arf*. However, when Myc levels were restored by using an siRNA-resistant (lacking the targeted 3′ UTR sequence) Myc-ER construct and 4-hydroxytamoxifen treatment (50), 47S transcript levels significantly increased in the *Arf*-null MEFs, suggesting that Myc proteins can positively direct rDNA transcription in the absence of ARF (Fig. 9A and B).

NPM is required for the growth gains seen in the absence of *Arf*. Having shown that nearly half of the basal ARF proteins are bound to NPM in wild-type MEFs (Fig. 7B), we hypothesized that NPM is a critical nucleolar target of basal ARF and that the loss of *Arf* resulted in unregulated NPM activities. To test this hypothesis, we knocked down NPM expression in MEFs lacking *Arf* to determine the effects on ribosome biogenesis and protein synthesis. Using lentiviruses carrying shRNAs targeting mouse NPM, we were able to achieve greater than 90% NPM knockdown efficiency (Fig. 10A). How-

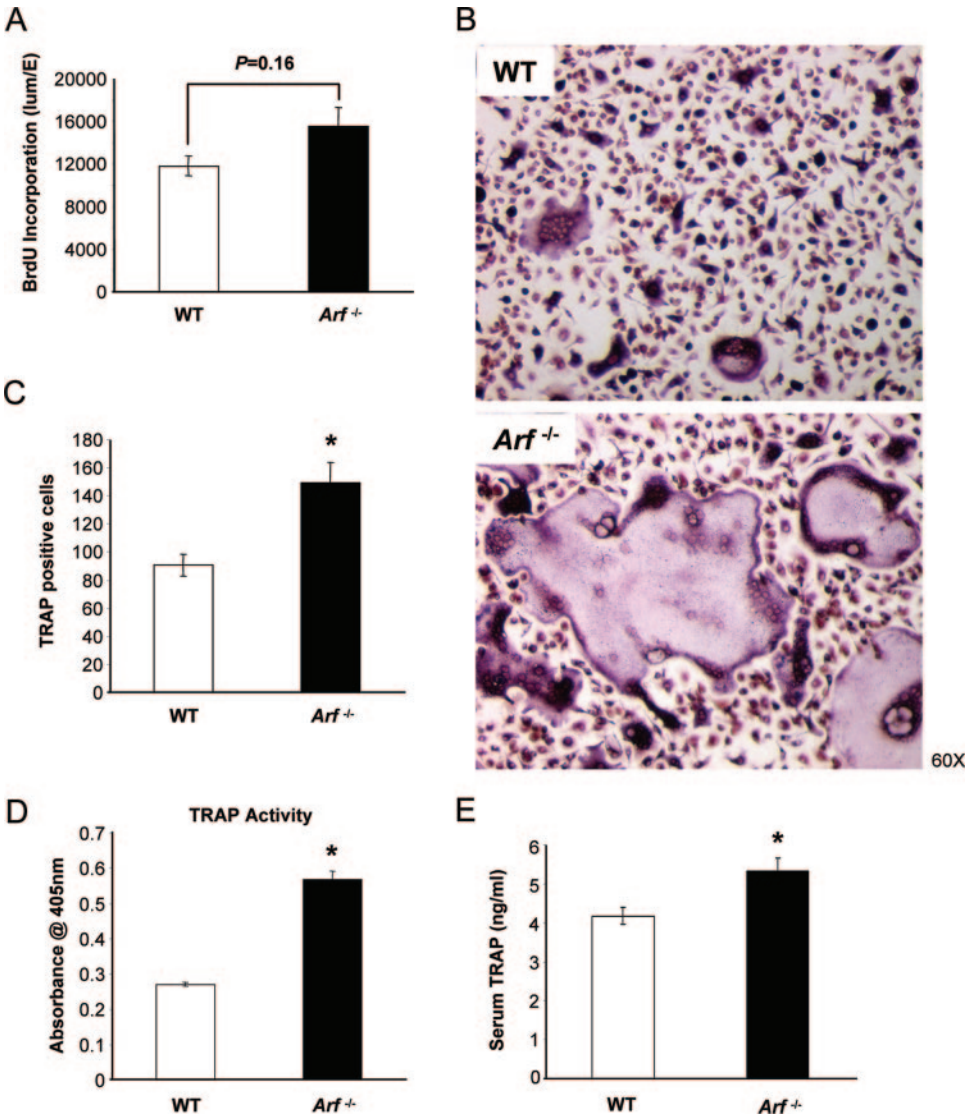

FIG. 6. Loss of $p19^{ARF}$ has functional consequences on osteoclast biology. (A) BrdU incorporation in the wild-type (WT) and $Arf^{-/-}$ macrophages. (B) Representative TRAP staining of equal numbers of BMMs following 3 days of treatment with M-CSF and RANKL reveals an increase in multinucleated osteoclasts formed from the $Arf^{-/-}$ precursors. (C) The graph shows increases in TRAP-positive osteoclasts with greater than five nuclei derived from the $Arf^{-/-}$ bone marrow. *, $P = 0.01$. (D) TRAP solution assay of equal numbers of TRAP-positive cells. Cells from the wild-type (day 4 post-RANKL addition) or the $Arf^{-/-}$ (day 3 post-RANKL addition) precursors were lysed and incubated in a colorimetric assay with *p*-nitrophenyl phosphate, a substrate for TRAP. The graph shows an A_{405}. *, $P = 0.01$. (E) Levels of serum TRAP 5b in $Arf^{-/-}$ compared to that in wild-type mice ($P = 0.03$; $n = 5$ mice in each group) as measured by ELISA.

ever, the reduction in NPM protein expression led to a dramatic increase in 47S rRNA transcripts in cells that also lacked *Arf* (Fig. 10B), indicating that NPM might actually inhibit rDNA transcription. The increase in 47S rRNA did not result in a similar increase in rRNA processing. In fact, we observed a slight but notable accumulation of 32S rRNA for cells lacking both ARF and NPM (Fig. 10C). We also noticed the appearance of an rRNA species above the 18S rRNA only in the absence of ARF and NPM, which may be the result of an additional processing defect (Fig. 10C). Furthermore, nuclear exportation of processed 18S rRNA was significantly attenuated (55% reduction) in the *Arf*-null cells lacking NPM (Fig. 10D), demonstrating the requirement for NPM in trafficking mature rRNAs out of the nucleus and into the cytosol. In response to decreased ribosome export to the cytosol, the $Arf^{-/-}$ MEFs with reduced NPM expression exhibited significantly attenuated protein synthesis rates (Fig. 10E). Thus, gains in rDNA transcription are not realized in terms of overall protein synthesis in the absence of NPM. This could be a result of a ribosome biogenesis feedback loop, where reduced ribosome export causes a shift in rDNA transcription to compensate for the lack of cytosolic ribosomes. However, in the absence of NPM, these ribosomes cannot be properly exported.

To determine whether protein synthesis gains observed with the absence of *Arf* were caused by the deregulation of NPM and were independent of proliferation, we lowered the levels

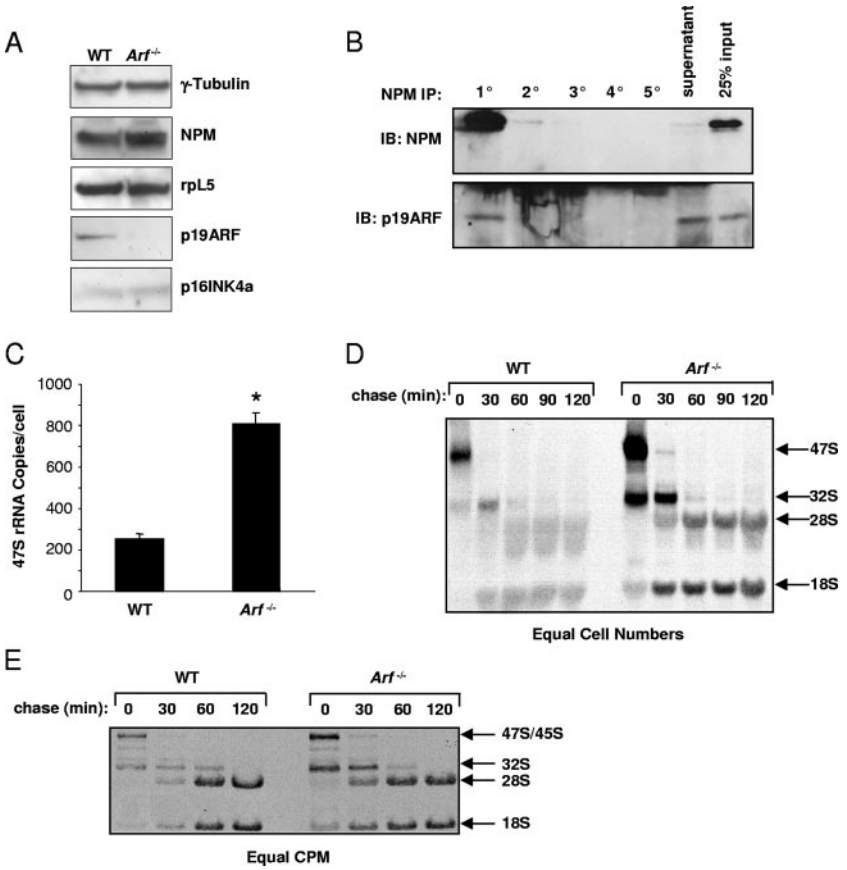

FIG. 7. ARF exerts its effects through the control of rRNA synthesis and processing. (A) Western blotting demonstrates that the *Arf*$^{-/-}$ MEFs do not have alterations in the levels of nucleolar proteins NPM and ribosomal protein L5. (B) Serial NPM immunoprecipitation. Wild-type cells were lysed and serially immunoprecipitated (five times) with mouse NPM antibodies. The final supernatant was concentrated and was included as a control for non-NPM binding proteins. (C) Total RNA was collected from equal numbers of asynchronously dividing cells, and quantitative real-time RT-PCR was performed with a primer specific to the mouse 47S transcript. (D) The wild-type (WT) and *Arf*$^{-/-}$ cells were pulsed with a [^{3}H]uridine label for 30 min, followed by a chase with label-free medium for the indicated times. Total RNA was isolated from equal cell numbers, loaded onto formaldehyde-containing agarose gels, and transferred to membranes for fluorography. (E) Cells were labeled with [*methyl*-^{3}H]methionine, followed by a chase with medium containing excess unlabeled methionine for the indicated times. Total RNA was isolated, and equal radioactive counts were loaded onto gels and transferred to membranes for fluorography. CPM, counts per minute.

of NPM in maturing osteoclasts. We reasoned that by reducing NPM expression in osteoclasts, we would mimic a restoration of ARF activity without the complicating effects of cell cycle arrest (i.e., osteoclasts are postmitotic) or of ARF binding to Mdm2 (i.e., a p53 response). This provided us with an experimental system with which to test the hypothesis that a balance exists between ARF and NPM in determining the ribosome output from the nucleolus. Lentiviral shRNAs targeting NPM in BMMs significantly reduced NPM protein expression levels (Fig. 11A). Concomitant with decreases in NPM expression, the *Arf*$^{-/-}$ osteoclasts were dramatically reduced in levels of TRAP staining (Fig. 11B) and activity (Fig. 11C), indicating a sensitivity of osteoclast differentiation to lower NPM levels. However, wild-type osteoclasts were far less sensitive to decreases in NPM expression, showing no statistically significant difference in TRAP activity. These data suggest that, in the absence of *Arf*, amplified ribosome biogenesis requires a set amount of NPM (for processing or export) and further implicates NPM as a target of basal ARF proteins in the maintenance of proper ribosome output.

DISCUSSION

While ARF has been long appreciated for its abilities to positively regulate p53 levels in the cell (22, 29) and serve as a sensor of hyperproliferative signals (19, 20, 31, 50), the relatively low abundance of ARF in interphase cells implied that ARF functioned only as a cellular checkpoint against aberrant growth and proliferation signals. In this manner, only signals powerful enough to elicit increases in ARF protein expression would trigger an actual ARF response. This implies that basal ARF molecules, even at their low levels, must be antagonized or held in check for the cell to undergo proper cell cycle progression and cell growth regimens. Teleologically, this model seems justified, given the genomic organization of the *Ink4a/Arf* locus where "leakiness" in p16INK4a or p19ARF

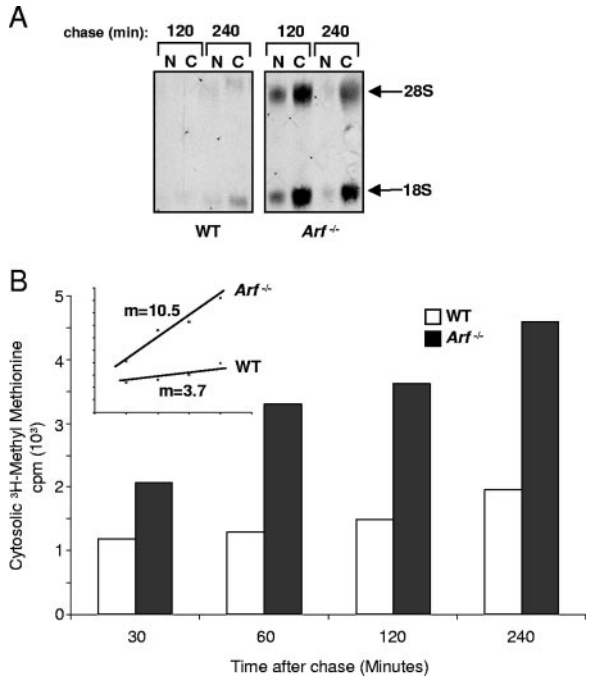

FIG. 8. Nucleocytoplasmic shuttling of newly synthesized ribosomes is enhanced in the absence of *Arf*. (A) Equal numbers of cells were pulsed with [*methyl*-^{3}H]methionine and chased with unlabeled methionine-containing medium for the indicated times. Total RNA was isolated from nuclear (N) and cytoplasmic (C) fractions and subjected to fluorography. (B) Cytoplasmic fractions from the indicated times were also subjected to liquid scintillation counting to obtain a quantitative estimate of total cytoplasmic rRNA. Inset, scatter plot of data presented in panel B with best-fit lines to indicate the velocity of export. m = slope. WT, wild type.

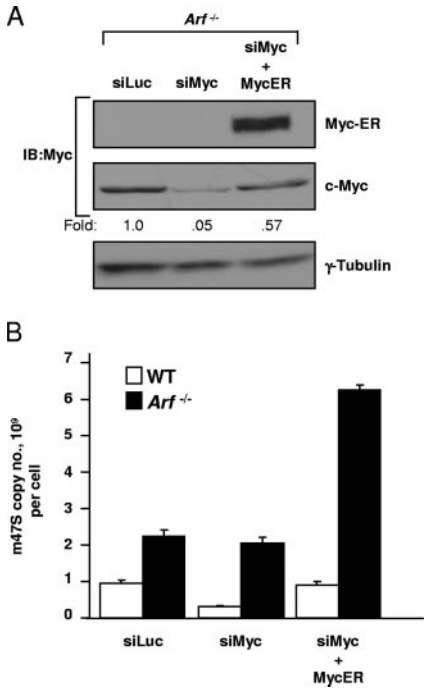

FIG. 9. Myc is not required for the enhanced rDNA transcription of the *Arf*-null MEFs. the $Arf^{-/-}$ MEFs (2×10^6) transduced with siLuc control siRNAs or Myc siRNAs in the absence or presence of Myc-ER expressing retroviruses and 4-hyrodxytamoxifen were harvested and (A) immunoblotted with antibodies recognizing c-Myc or γ-tubulin. (B) RNA was isolated from the above cells and real-time PCR using 47S rRNA probes was performed in triplicate. WT, wild type.

transcription would have dire effects on the growth and survival of the cell (14). It is widely held that this locus is repressed in mice and that only under conditions of extreme stress or oncogenic signaling is the locus transcribed to elicit a growth and proliferative arrest phenotype (51). Here, we provide evidence that the physiologically low level of ARF has a regulatory role in nucleolar function and ribosome biogenesis. Indeed, as early as 4 days post-ARF knockdown by lentiviral shRNA infection, we observed changes in nucleolar morphology and function that are reminiscent of data from the $Arf^{-/-}$ embryonic cells. This strongly supports the hypothesis that basal ARF consistently monitors and dynamically alters the nucleolar growth/suppression pathway on a day-to-day basis. We would now argue that basal ARF proteins must be maintained at some steady-state level to provide constant surveillance of nucleolar function. Given the great energy demands of the nucleolus (ribosome biogenesis and protein synthesis account for nearly 50% of the cell's energy), dysfunctional nucleolar processes may need to be adjusted at a moment's notice (26). In support of this contention, a recent report (33) demonstrated that selective disruption of the nucleolus by either UV radiation or a number of "stress" responses induced cell cycle arrest and markedly enhanced p53 stability. While we did not observe any gross disruption of nucleoli in cells either lacking or overexpressing ARF, we did observe numerous qualitative changes in the size and number of nucleoli in cells lacking *Arf*. This would suggest that basal ARF might play a vital role in determining the protein composition of nucleoli, acting to prevent the release of specific ribosomal proteins from the nucleolus or to prohibit the entrance of unwanted (potentially oncogenic) nuclear proteins into the nucleolus.

In the past few years, numerous p53-independent functions have been ascribed to ARF (35). We found that nearly half of the basal ARF in the cell is in a complex with NPM, a protein previously shown to interact with human and mouse ARF proteins (4, 8, 21). While much of the work concerning the ARF-NPM interaction has focused on the ability of each protein to antagonize the function of the other (4, 8, 21, 24, 46), our findings suggest that the baseline interaction functions to maintain a controlled level of ribosome biogenesis. We propose a model where basal ARF antagonizes a small pool of NPM, either directly or enzymatically (8, 38), and thereby constantly limits ribosome output from the nucleolus. Importantly, levels of NPM did not change in the absence of ARF, but rather NPM activity was greatly increased as measured by its ability to promote ribosome nuclear export. Consistent with this model, the knockdown of basal NPM proteins resulted in dramatic reductions in protein production independent of cell proliferation, again underscoring the need for a consistent level of "ARF-free" NPM to promote ribosome synthesis.

While the mechanism and nature of such inhibition are still unclear, our data are consistent with a "thermostat" function for ARF, in that small changes in the abundance of ARF cause

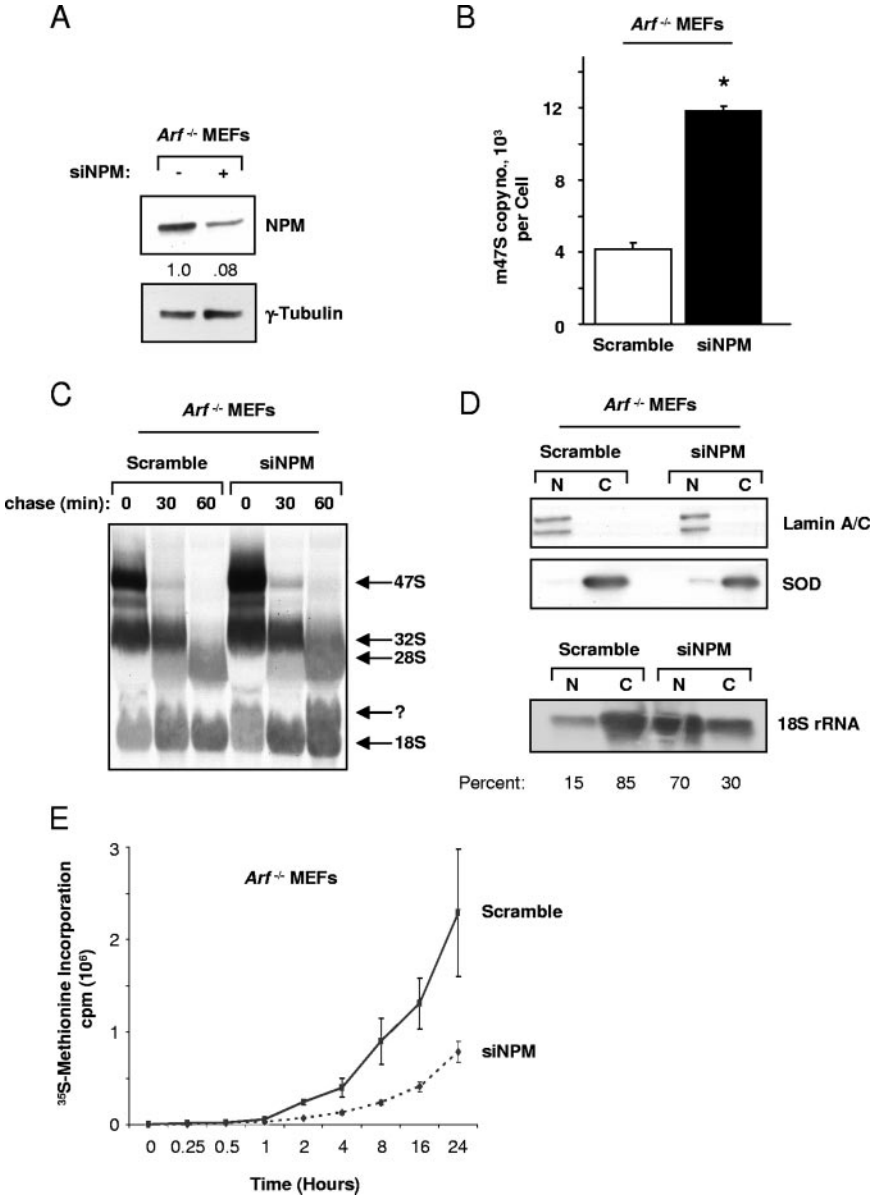

FIG. 10. NPM is required for ribosome gains in the absence of *Arf*. The $Arf^{-/-}$ MEFs (2×10^6) infected with lentiviruses encoding scrambled or NPM shRNAs were (A) lysed and immunoblotted with antibodies recognizing NPM and γ-tubulin; (B) lysed and RNA isolated for real-time PCR using 47S rRNA probes; (C) labeled with [*methyl*-^{3}H]methionine, followed by a chase with medium containing excess unlabeled methionine for the indicated times, isolation of total RNA and equal radioactive counts, loading onto gels, and transfer to membranes for fluorography; (D) fractionated into nuclear (N) and cytosolic (C) lysates and immunoblotted with lamin A/C and SOD or Northern blotted with probes recognizing the 18S rRNA; or (E) starved of methionine and cysteine for 30 min prior to the addition of label for the indicated times, followed by lysis, trichloroacetic acid precipitation of proteins, and liquid scintillation counting. *, $P < 0.01$.

its binding partners to either dampen or enhance ribosome synthesis and export and, ultimately, lead to global changes in protein synthesis. It is apparent from our data that basal ARF can act in three distinct steps: (i) rDNA transcription, (ii) rRNA processing, and (iii) rRNA nuclear export.

While NPM has been ascribed roles in both rRNA processing and nuclear export (36, 47), we are uncertain of its ability to regulate rDNA transcription. In fact, NPM and ARF are both found in the granular region of the nucleolus, relatively far removed from the sites of nucleolar rDNA transcription (8). However, we did observe significantly enhanced transcription of 47S rRNA in the absence of *Arf*, implying that ARF proteins might regulate this process either directly or indirectly. This is not unprecedented, given recent findings that human ARF interacts with topoisomerase I to inhibit rDNA transcription (3, 23). Additionally, nearly half of the basal ARF protein is not bound to NPM, and we therefore cannot rule out the possibility that this pool of ARF is bound to proteins involved in rDNA transcription.

We suggest that ARF is expressed at a low level in interphase cells to ensure that proper growth control is achieved. This would serve to keep the cell in metabolic check, prevent-

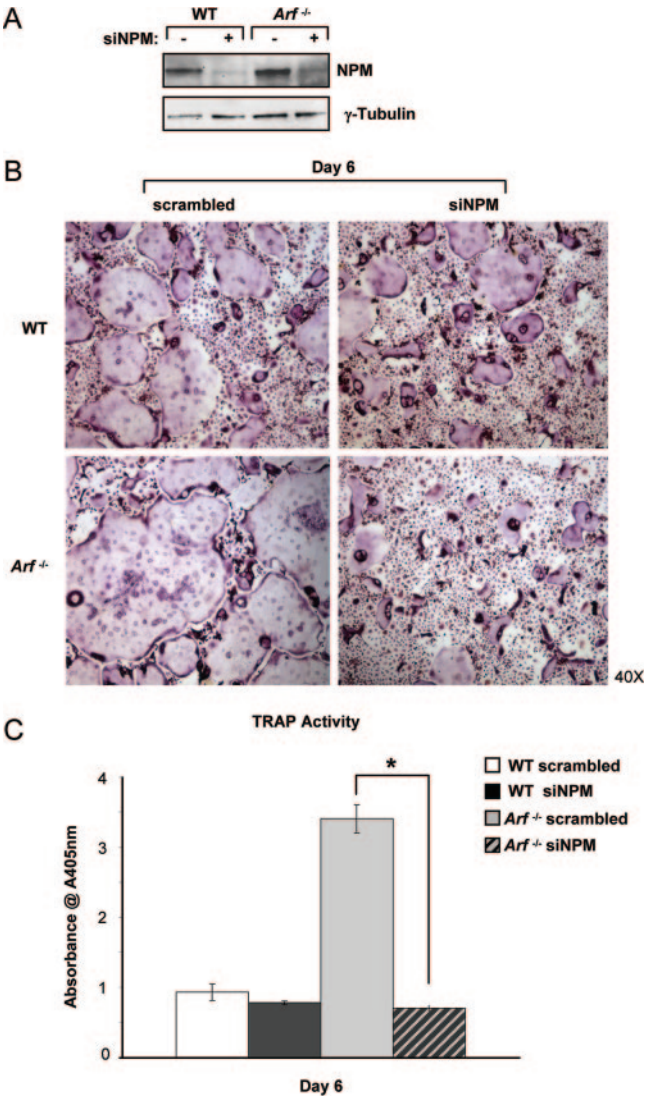

FIG. 11. Loss of NPM expression inhibits osteoclastogenesis in the $Arf^{-/-}$ cells. (A) Western blotting of macrophages infected with either control or lentivirus-targeted shRNA specific to NPM to confirm the gene knockdown. (B) TRAP staining of osteoclasts differentiated in vitro with RANKL and M-CSF for 6 days. (C) TRAP activity assay of equal numbers of osteoclasts from the indicated genotypes. *, $P < 0.01$. WT, wild type.

ing the cell from wasting energy on unnecessary protein synthesis. Disruption of this exquisite basal ARF control would then have a twofold effect: (i) cells would produce far too many ribosomes, resulting in tremendous gains in protein synthesis, and (ii) the resultant cells would be highly susceptible to oncogenic signals. This setting would seem to provide a selective advantage to premalignant cells by ramping up their growth and, in the presence of appropriate signals, their proliferation. In support of this hypothesis, a recent study on the methylation of key loci involved in colorectal carcinogenesis demonstrated that 32% of the adenomas (premalignant lesions) isolated from patients with sporadic colorectal cancer demonstrated abnormalities at the *Arf* locus (11). Our findings represent a novel and important role for basal ARF in maintaining protein synthetic homeostasis in nonmalignant cells. While NPM is certainly required for much of the ribosome biogenesis gains observed for *Arf*-deficient cells, other interesting nucleolar targets of basal ARF must certainly exist. Precise details of how they may be affected remain elusive. Understanding the nucleolar integration of disparate requirements for proliferation, growth, and ribosome biogenesis will deepen our knowledge of how proteins like ARF adapted from regulators of cellular homeostasis to bona fide tumor suppressors.

ACKNOWLEDGMENTS

We thank Martine Roussel, Charles Sherr, Tyler Jacks, and Gerard Zambetti for plasmids, antibodies, and mice, as well as Michael Benjamin for excellent assistance. We are extremely grateful to Sheila Stewart, Phil Stahl, Arie Perry, and Josh Rubin for insightful discussions.

A.J.A. is a recipient of a grant-in-aid from the Department of Defense Breast Cancer Research Program (BC030793). L.B.M. is supported by the Department of Defense Prostate Cancer Research Program award number W81XWH-04-0909. A.J.S. and M.K. are supported by the Siteman Cancer Biology Pathway. J.D.W. thanks the Pew Charitable Trusts and is a recipient of grants-in-aid from the Susan G. Komen for the Cure and National Institutes of Health (GM066032).

REFERENCES

1. **Aubele, M., S. Biesterfeld, M. Derenzini, P. Hufnagl, H. Martin, D. Ofner, D. Ploton, and J. Ruschoff for the Committee on AgNOR Quantitation within the European Society of Pathology.** 1994. Guidelines of AgNOR quantitation. Zentralbl. Pathol. **140:**107–108.
2. **Ayrault, O., L. Andrique, D. Fauvin, B. Eymin, S. Gazzeri, and P. Seite.** 2006. Human tumor suppressor p14ARF negatively regulates rRNA transcription and inhibits UBF1 transcription factor phosphorylation. Oncogene **25:**7577–7786.
3. **Ayrault, O., L. Andrique, C. J. Larsen, and P. Seite.** 2004. Human Arf tumor suppressor specifically interacts with chromatin containing the promoter of rRNA genes. Oncogene **23:**8097–8104.
4. **Bertwistle, D., M. Sugimoto, and C. J. Sherr.** 2004. Physical and functional interactions of the Arf tumor suppressor protein with nucleophosmin/B23. Mol. Cell. Biol. **24:**985–996.
5. **Bertwistle, D., F. Zindy, C. J. Sherr, and M. F. Roussel.** 2004. Monoclonal antibodies to the mouse p19(Arf) tumor suppressor protein. Hybrid. Hybridomics **23:**293–300.
6. **Birnstiel, M. L., M. I. Chipchase, and B. B. Hyde.** 1963. The nucleolus, a source of ribosomes. Biochim. Biophys. Acta **76:**454–462.
7. **Boon, K., H. N. Caron, R. van Asperen, L. Valentijn, M. C. Hermus, P. van Sluis, I. Roobeek, I. Weis, P. A. Voute, M. Schwab, and R. Versteeg.** 2001. N-myc enhances the expression of a large set of genes functioning in ribosome biogenesis and protein synthesis. EMBO J. **20:**1383–1393.
8. **Brady, S. N., Y. Yu, L. B. Maggi, Jr., and J. D. Weber.** 2004. ARF impedes NPM/B23 shuttling in an Mdm2-sensitive tumor suppressor pathway. Mol. Cell. Biol. **24:**9327–9338.
9. **Ciarmatori, S., P. H. Scott, J. E. Sutcliffe, A. McLees, H. M. Alzuherri, J. H. Dannenberg, H. te Riele, I. Grummt, R. Voit, and R. J. White.** 2001. Overlapping functions of the pRb family in the regulation of rRNA synthesis. Mol. Cell. Biol. **21:**5806–5814.
10. **Cui, C., and H. Tseng.** 2004. Estimation of ribosomal RNA transcription rate in situ. BioTechniques **36:**134–138.
11. **Esteller, M., S. Tortola, M. Toyota, G. Capella, M. A. Peinado, S. B. Baylin, and J. G. Herman.** 2000. Hypermethylation-associated Inactivation of p14ARF is independent of p16INK4a methylation and p53 mutational status. Cancer Res. **60:**129–133.
12. **Fingar, D. C., and J. Blenis.** 2004. Target of rapamycin (TOR): an integrator of nutrient and growth factor signals and coordinator of cell growth and cell cycle progression. Oncogene **23:**3151–3171.
13. **Fromont-Racine, M., B. Senger, C. Saveanu, and F. Fasiolo.** 2003. Ribosome assembly in eukaryotes. Gene **313:**17–42.
14. **Gil, J., and G. Peters.** 2006. Regulation of the INK4b-ARF-INK4a tumour suppressor locus: all for one or one for all. Nat. Rev. Mol. Cell. Biol. **7:**667–677.
15. **Grandori, C., N. Gomez-Roman, Z. A. Felton-Edkins, C. Ngouenet, D. A. Galloway, R. N. Eisenman, and R. J. White.** 2005. c-Myc binds to human ribosomal DNA and stimulates transcription of rRNA genes by RNA polymerase I. Nat. Cell Biol. **7:**311–318.
16. **Grewal, S. S., L. Li, A. Orian, R. N. Eisenman, and B. A. Edgar.** 2005. Myc-dependent regulation of ribosomal RNA synthesis during Drosophila development. Nat. Cell Biol. **7:**295–302.

17. **Hannan, K. M., R. D. Hannan, S. D. Smith, L. S. Jefferson, M. Lun, and L. I. Rothblum.** 2000. Rb and p130 regulate RNA polymerase I transcription: Rb disrupts the interaction between UBF and SL-1. Oncogene **19:**4988–4999.
18. **Hernandez-Verdun, D., and P. Roussel.** 2003. Regulators of nucleolar functions. Prog. Cell Cycle Res. **5:**301–308.
19. **Inoue, K., M. F. Roussel, and C. J. Sherr.** 1999. Induction of ARF tumor suppressor gene expression and cell cycle arrest by transcription factor DMP1. Proc. Natl. Acad. Sci. USA **96:**3993–3998.
20. **Inoue, K., R. Wen, J. E. Rehg, M. Adachi, J. L. Cleveland, M. F. Roussel, and C. J. Sherr.** 2000. Disruption of the ARF transcriptional activator DMP1 facilitates cell immortalization, Ras transformation, and tumorigenesis. Genes Dev. **14:**1797–1809.
21. **Itahana, K., K. P. Bhat, A. Jin, Y. Itahana, D. Hawke, R. Kobayashi, and Y. Zhang.** 2003. Tumor suppressor ARF degrades B23, a nucleolar protein involved in ribosome biogenesis and cell proliferation. Mol. Cell **12:**1151–1164.
22. **Kamijo, T., F. Zindy, M. F. Roussel, D. E. Quelle, J. R. Downing, R. A. Ashmun, G. Grosveld, and C. J. Sherr.** 1997. Tumor suppression at the mouse INK4a locus mediated by the alternative reading frame product p19ARF. Cell **91:**649–659.
23. **Karayan, L., J. F. Riou, P. Seite, J. Migeon, A. Cantereau, and C. J. Larsen.** 2001. Human ARF protein interacts with topoisomerase I and stimulates its activity. Oncogene **20:**836–848.
24. **Korgaonkar, C., J. Hagen, V. Tompkins, A. A. Frazier, C. Allamargot, F. W. Quelle, and D. E. Quelle.** 2005. Nucleophosmin (B23) targets ARF to nucleoli and inhibits its function. Mol. Cell. Biol. **25:**1258–1271.
25. **Maggi, L. B., Jr., and J. D. Weber.** 2005. Nucleolar adaptation in human cancer. Cancer Investig. **23:**599–608.
26. **Moss, T.** 2004. At the crossroads of growth control; making ribosomal RNA. Curr. Opin. Genet. Dev. **14:**210–217.
27. **Pelletier, C. L., L. B. Maggi, Jr., S. N. Brady, D. K. Scheidenhelm, D. H. Gutmann, and J. D. Weber.** 2007. TSC1 sets the rate of ribosome export and protein synthesis through nucleophosmin translation. Cancer Res. **67:**1609–1617.
28. **Pich, A., L. Chiusa, and E. Margaria.** 2000. Prognostic relevance of AgNORs in tumor pathology. Micron **31:**133–141.
29. **Pomerantz, J., N. Schreiber-Agus, N. J. Liegeois, A. Silverman, L. Alland, L. Chin, J. Potes, K. Chen, I. Orlow, H. W. Lee, C. Cordon-Cardo, and R. A. DePinho.** 1998. The Ink4a tumor suppressor gene product, p19Arf, interacts with MDM2 and neutralizes MDM2's inhibition of p53. Cell **92:**713–723.
30. **Qi, Y., M. A. Gregory, Z. Li, J. P. Brousal, K. West, and S. R. Hann.** 2004. p19ARF directly and differentially controls the functions of c-Myc independently of p53. Nature **431:**712–717.
31. **Ries, S., C. Biederer, D. Woods, O. Shifman, S. Shirasawa, T. Sasazuki, M. McMahon, M. Oren, and F. McCormick.** 2000. Opposing effects of Ras on p53: transcriptional activation of mdm2 and induction of p19ARF. Cell **103:**321–330.
32. **Ritossa, F. M., and S. Spiegelman.** 1965. Localization of DNA complementary to ribosomal RNA in the nucleolus organizer region of Drosophila melanogaster. Proc. Natl. Acad. Sci. USA **53:**737–745.
33. **Rubbi, C. P., and J. Milner.** 2003. Disruption of the nucleolus mediates stabilization of p53 in response to DNA damage and other stresses. EMBO J. **22:**6068–6077.
34. **Ruggero, D., and P. P. Pandolfi.** 2003. Does the ribosome translate cancer? Nat. Rev. Cancer **3:**179–192.
35. **Sherr, C. J.** 2006. Divorcing ARF and p53: an unsettled case. Nat. Rev. Cancer **6:**663–673.
36. **Spector, D. L., R. L. Ochs, and H. Busch.** 1984. Silver staining, immunofluorescence, and immunoelectron microscopic localization of nucleolar phosphoproteins B23 and C23. Chromosoma **90:**139–148.
37. **Sugimoto, M., M. L. Kuo, M. F. Roussel, and C. J. Sherr.** 2003. Nucleolar Arf tumor suppressor inhibits ribosomal RNA processing. Mol. Cell **11:**415–424.
38. **Tago, K., S. Chiocca, and C. J. Sherr.** 2005. Sumoylation induced by the Arf tumor suppressor: a p53-independent function. Proc. Natl. Acad. Sci. USA **102:**7689–7694.
39. **Tao, W., and A. J. Levine.** 1999. P19(ARF) stabilizes p53 by blocking nucleocytoplasmic shuttling of Mdm2. Proc. Natl. Acad. Sci. USA **96:**6937–6941.
40. **Tapon, N., K. H. Moberg, and I. K. Hariharan.** 2001. The coupling of cell growth to the cell cycle. Curr. Opin. Cell Biol. **13:**731–737.
41. **Teitelbaum, S. L., and F. P. Ross.** 2003. Genetic regulation of osteoclast development and function. Nat. Rev. Genet. **4:**638–649.
42. **Trere, D.** 2000. AgNOR staining and quantification. Micron **31:**127–131.
43. **Voit, R., K. Schafer, and I. Grummt.** 1997. Mechanism of repression of RNA polymerase I transcription by the retinoblastoma protein. Mol. Cell. Biol. **17:**4230–4237.
44. **Weber, J. D., M. L. Kuo, B. Bothner, E. L. DiGiammarino, R. W. Kriwacki, M. F. Roussel, and C. J. Sherr.** 2000. Cooperative signals governing ARF-Mdm2 interaction and nucleolar localization of the complex. Mol. Cell. Biol. **20:**2517–2528.
45. **Weber, J. D., L. J. Taylor, M. F. Roussel, C. J. Sherr, and D. Bar-Sagi.** 1999. Nucleolar Arf sequesters Mdm2 and activates p53. Nat. Cell. Biol. **1:**20–26.
46. **Yu, Y., L. B. Maggi, Jr., S. N. Brady, A. J. Apicelli, M. S. Dai, H. Lu, and J. D. Weber.** 2006. Nucleophosmin is essential for ribosomal protein L5 nuclear export. Mol. Cell. Biol. **26:**3798–3809.
47. **Yung, B. Y., R. K. Busch, H. Busch, A. B. Mauger, and P. K. Chan.** 1985. Effects of actinomycin D analogs on nucleolar phosphoprotein B23 (37,000 daltons/pI 5.1). Biochem. Pharmacol. **34:**4059–4063.
48. **Zhai, W., and L. Comai.** 2000. Repression of RNA polymerase I transcription by the tumor suppressor p53. Mol. Cell. Biol. **20:**5930–5938.
49. **Zhao, H., H. Kitaura, M. S. Sands, F. P. Ross, S. L. Teitelbaum, and D. V. Novack.** 2005. Critical role of beta3 integrin in experimental postmenopausal osteoporosis. J. Bone Miner. Res. **20:**2116–2123.
50. **Zindy, F., C. M. Eischen, D. H. Randle, T. Kamijo, J. L. Cleveland, C. J. Sherr, and M. F. Roussel.** 1998. Myc signaling via the ARF tumor suppressor regulates p53-dependent apoptosis and immortalization. Genes Dev. **12:**2424–2433.
51. **Zindy, F., R. T. Williams, T. A. Baudino, J. E. Rehg, S. X. Skapek, J. L. Cleveland, M. F. Roussel, and C. J. Sherr.** 2003. Arf tumor suppressor promoter monitors latent oncogenic signals in vivo. Proc. Natl. Acad. Sci. USA **100:**15930–15935.